Available online at www.sciencedirect.com
SCIENCE DIRECT®
Ocean Modelling 6 (2004) 405–422
Ocean Modelling
www.elsevier.com/locate/omodol

Inverse modeling of discrete interaction approximations for nonlinear interactions in wind waves ☆

Hendrik L. Tolman *

SAIC-GSO at NOAA/NCEP/EMC Marine Modeling and Analysis Branch, 5200 Auth Road, Room 209, Camp Springs, MD 20746, USA

Received 16 April 2003; received in revised form 11 July 2003; accepted 9 September 2003

Abstract

In the last two decades, the Discrete Interaction Approximation (DIA) has been the only economically feasible parameterization for nonlinear wave–wave interactions in operational wind wave models. Its major drawback is its limited accuracy. Several improvements to the DIA have been suggested recently. The present study summarizes these improvements and suggests some new modifications to the DIA. Using inverse modeling techniques, where the potential of various DIAs is assessed by optimal fitting to exact solutions, a comprehensive comparison of the potential of several such improvements is made. An in depth analysis of the behavior of DIAs in full wave models will be the subject of a second study, to be reported elsewhere. The major findings of this study are that: (i) An expanded definition of the representative quadruplet with additional degrees of freedom is necessary for an accurate representation of the exact interactions; (ii) Slowly varying the free parameters in such a DIA as a function of the spectral frequency f results in a (mostly qualitative) improvement; (iii) A DIA with expanded quadruplet definition and with four representative quadruplets is found to reproduce the exact source term accurately; (iv) Adding additional tunable constants to the equation for the strength of the interactions has little impact on the quality of the DIA.

Keywords: Wind waves; Nonlinear interactions; Numerical modeling

☆ MMAB contribution Nr. 230.

* Tel.: +1-301-763-8000x7253; fax: +1-301-763-8545.
E-mail address: hendrik.tolman@noaa.gov (H.L. Tolman).

1463-5003/$ - see front matter
doi:10.1016/j.ocemod.2003.09.002

1. Introduction

Ocean waves generated by winds are conventionally described with an energy spectrum $F(f,\theta)$, which describes the distribution of wave energy over spectral frequencies f and directions θ. In its simplest form, the evolution of such a spectrum is described by the following spectral balance equation (Hasselmann, 1960):

$$\frac{\mathrm{D}F}{\mathrm{D}t} = S_{\mathrm{tot}} = S_{\mathrm{in}} + S_{\mathrm{nl}} + S_{\mathrm{ds}}, \tag{1}$$

where the total derivative includes effects of wave propagation, and S_{tot} represents the net sources and sinks of wave energy. The elementary sources and sinks of wave energy are the wind input (S_{in}), the nonlinear interactions (S_{nl}), and the dissipation (S_{ds}) source terms.

The nonlinear interactions represent a mechanism for shifting wave energy to lower frequencies, and are, therefore, critical in describing the growth of wind waves (e.g., Hasselmann et al., 1973). The basic form of the interactions has been established more than 40 years ago (Phillips, 1960; Hasselmann, 1962, 1963a,b). Reviews of the interactions and their impact can be found, for instance, in Masuda (1980), Phillips (1981), Young and Van Vledder (1993) or Komen et al. (1994). The comprehensive wave model intercomparison performed in the Sea Wave Modeling Project (SWAMP, SWAMP group, 1985) identified the need for numerical wave models to evaluate S_{nl} explicitly. Such a model with an explicit parameterization of S_{nl} and without presumed spectral shapes is known as a third-generation wave model.

The nonlinear interactions source term describes the resonant exchange of energy, momentum and action between four spectral components (quadruplets) with wavenumber vectors $\vec{k}_1$ through $\vec{k}_4$ and (radian) frequencies σ_1 through σ_4 ($\sigma = 2\pi f$). The quadruplets exchange energy whenever they satisfy the resonance conditions (Hasselmann, 1962, 1963a):

$$\vec{k}_1 + \vec{k}_2 = \vec{k}_3 + \vec{k}_4, \tag{2}$$

$$\sigma_1 + \sigma_2 = \sigma_3 + \sigma_4. \tag{3}$$

The interactions are conventionally expressed in terms of the rate of change of the action spectrum $n \equiv F/\sigma$ in terms of the wavenumber vector $\vec{k}$, as

$$\frac{\partial n_1}{\partial t} = \int\int\int G(\vec{k}_1,\vec{k}_2,\vec{k}_3,\vec{k}_4)\delta_k\delta_\sigma[n_1 n_3(n_4 - n_2) + n_2 n_4(n_3 - n_1)]\,\mathrm{d}\vec{k}_2\,\mathrm{d}\vec{k}_3\,\mathrm{d}\vec{k}_4, \tag{4}$$

where n_i is the action density at component i, $n_i = n(\vec{k}_i)$, G is a complex coupling coefficient (Webb, 1978; Herterich and Hasselmann, 1980), and δ_k and δ_σ are delta functions corresponding to the resonance conditions (2) and (3). Singularities in G and the sixfold integral in (4) make the numerical solution of the latter equation (and hence of S_{nl}) several orders of magnitude more expensive than all other aspects of a numerical solution of Eq. (1) combined. It is therefore not feasible to use such an algorithm in operational wave models.

With the development of the Discrete Interaction Approximation (DIA, Hasselmann et al., 1985), it became possible for the first time to develop an economically feasible third-generation wave model (WAM, WAMDIG, 1988). Details of the DIA, including ways in which the DIA attains economical feasibility, will be presented in Section 2. For practical applications, all present third-generation models still use some form of the DIA.

At the introduction of the DIA, its shortcomings were well documented (Hasselmann et al., 1985). Since then, several modifications to the DIA have been suggested to improve its performance, as will be discussed in Section 2. Such methods generally are more computationally expensive than the original DIA, by up to an order of magnitude. With recent advances in computer technology, such an increase in costs is rapidly becoming feasible for operational models, and therefore acceptable.

The present study presents an assessment of the capability of various DIAs to represent the exact nonlinear interaction source term S_{nl} for selected test cases. This assessment is made by means of inverse modeling, i.e., by optimization of the free parameters in each DIA. This optimization results in an objective or quantitative error measure for each DIA. A subjective or qualitative assessment proved important too, in particular to identify spurious elements in the interactions. Most previously suggested DIAs will be considered, as well as some new modified versions (see Section 2). Because S_{nl} is mainly important in the context of wave growth, test cases are limited to spectra that are representative for wind seas; additional swell fields will not be considered here. For simplicity, only deep water will be considered. The test cases considered are described in Section 3, and the corresponding results are presented in Section 4. For conciseness, only selected results will be presented here. A complete accounting of all test results obtained for this study is presented in Tolman (2003, henceforth denoted as T03). A discussion and conclusions are presented in Sections 5 and 6, respectively.

Due to the highly nonlinear nature of the interactions, it is not guaranteed that accurate interactions for a limited number of spectra will result in accurate model integration. Similarly, inaccurate interactions for individual spectra do not automatically lead to unacceptable model behavior. The latter was illustrated in Hasselmann et al. (1985), where the the original DIA with its limited accuracy for test spectra resulted in acceptable wave model behavior. Similarly, a simple time integration test presented in T03 shows that, contrary to common belief, a DIA that more accurately describes interactions for selected spectra can actually result in unrealistic model behavior. This illustrates the necessity of addressing the behavior of any interaction approximation as an integral part of a comprehensive wave model. The second part of this study, to be presented elsewhere, will address this issue in depth. The present study is intended to make a first selection of DIAs to be considered in more detail in the second study.

2. Discrete Interaction Approximations

In the original DIA of Hasselmann et al. (1985), a dramatic increase in computational speed relative to the numerical solution of the full Eqs. (2)–(4) is achieved in two ways. First, the multidimensional integration in Eq. (4) is replaced by the calculation of interactions for a single representative quadruplet only. This quadruplet satisfies the resonance conditions (2) and (3), as well as

$$\left.\begin{aligned} \vec{k}_2 &= \vec{k}_1 \\ \sigma_2 &= \sigma_1 \\ \sigma_3 &= (1+\lambda)\sigma_1 \\ \sigma_4 &= (1+\lambda)\sigma_1 \end{aligned}\right\}, \tag{5}$$

where λ is a constant. Separate nonlinear contributions δS_{nl} are calculated for $\vec{k}_1$ corresponding to each discrete spectral component. The full source term S_{nl} becomes the composite of all contributions. Note that for each $\vec{k}_1$, only two (mirror image) quadruplets satisfy Eqs. (2), (3) and (5).

Second, the DIA replaces the full integration in Eq. (4) with a discrete analogue (Hasselmann et al., 1985, Eq. (5.4)). After the proper Jacobean transformations are applied, the conventional DIA expression for contributions to δS_{nl} for all components of the quadruplet become (see Hasselmann et al., 1985; Van Vledder, 2001):

$$\begin{pmatrix} \delta S_{\mathrm{nl},1} \\ \delta S_{\mathrm{nl},3} \\ \delta S_{\mathrm{nl},4} \end{pmatrix} = \begin{pmatrix} -2 \\ 1 \\ 1 \end{pmatrix} C g^{-4} f_1^{11} \left[F_1^2 \left(\frac{F_3}{(1+\lambda)^4} + \frac{F_4}{(1-\lambda)^4} \right) - \frac{2F_1F_3F_4}{(1-\lambda^2)^4} \right], \tag{6}$$

where C is a constant, g is the acceleration of gravity, and $F_1 = F(f_1, \theta_1)$, etc. A speed up is gained here, because the complex coupling coefficient G with its singularities is no longer evaluated explicitly. Note that this expression implies a discrete spectral frequency grid where $f_{j+1} = \alpha f_j$ (with typicality $\alpha = 1.1$), and that it is constructed assuming deep water conditions. The restriction to deep water does not impact the present feasibility study, but needs to be addressed when a DIA is implemented in a wave model.

The DIA retains the conservation properties of the exact interactions. The distribution of the contributions $\delta S_{\mathrm{nl},1}$ through $\delta S_{\mathrm{nl},4}$ over the four components of the quadruplet in Eq. (6) guarantees the conservation of the total energy within the spectrum. If the conservation of energy is thus assured, the resonance conditions implicit to the definition of the quadruplet in turn guarantee the conservation of momentum and action (e.g., Hasselmann, 1963a; Webb, 1978). This implies that a DIA will have proper conservation properties regardless of the layout and number of quadruplets, as long as each quadruplet satisfies the resonance conditions. This furthermore implies that the conservation properties are retained regardless of the actual form of the common factors and the term in square brackets at the right side of Eq. (6).

In Hasselmann et al. (1985) and in the WAM model, the two free parameters in the DIA are set (by optimization) to $\lambda = 0.25$ and $C = 3 \times 10^7$. Such a DIA defined by Eqs. (2), (3), (5) and (6) will henceforth be denoted as the original DIA. Three types of modifications for the original DIA have been suggested: (i) the use of more than one representative quadruplet; (ii) alternative definitions of the representative quadruplet; (iii) alternative versions of equation for the discrete contributions (6).

Using a number of representative interaction configurations instead of exactly one, represents a natural way to increase the versatility of the DIA. It appears that approaches with two representative layouts for the quadruplet have been considered when developing the WAM model, and for other early third-generation wave models, but no formal documentation to corroborate this has been found by the present author. Recent approaches with multiple representative quadruplets are reported by Ueno and Ishizaka (1997), Van Vledder et al. (2000), and Hashimoto and Kawaguchi (2001). If $S_{\mathrm{nl},j}(f, \theta)$ represents the DIA contribution for representative quadruplet j, and N is the total number of representative quadruplets, such a multiple DIA can be defined as

$$S_{\mathrm{nl}}(f, \theta) = \frac{1}{N} \sum_{j=1}^{N} S_{\mathrm{nl},j}(f, \theta). \tag{7}$$

The factor $1/N$ is not strictly necessary and is omitted by previous authors. It assures that a multiple DIA composed of identical components becomes identical to its component, and thus results in a more transparent transition from single to multiple DIAs.

The representative quadruplet defined by the single parameter λ in Eq. (5) is restrictive, because it allows for only a small subset of possible quadruplet geometries. Van Vledder (2001) suggests an alternative quadruplet layout defined by three parameters, that can reproduce any possible layout of the quadruplet (see also T03 for details). In the present study, a new two-parameter quadruplet layout has been used, defined as

$$\left.\begin{aligned} &\vec{k}_1 + \vec{k}_2 = \vec{k}_3 + \vec{k}_4 = 2\vec{k} \\ &\sigma_1 = (1+\mu)\sigma \\ &\sigma_2 = (1-\mu)\sigma \\ &\sigma_3 = (1+\lambda)\sigma \\ &\sigma_4 = (1-\lambda)\sigma \end{aligned}\right\}, \tag{8}$$

where λ and μ, are the free parameters defining the layout of the quadruplet, and which is evaluated for each $(\vec{k},\sigma)$ of the discrete spectral grid. Four solutions satisfy Eq. (8), whereas only two satisfy Eq. (5). Note that this quadruplet definition is less versatile than the definition of Van Vledder (2001). However, because it proved sufficiently versatile in the numerical experiments, it was deemed adequate for the present study.

The third published modification (Ueno and Ishizaka, 1997) adds individual constants to selected terms in the square brackets in Eq. (6). The corresponding equation for contributions to S_{nl}, including multiple representative quadruplets, and accounting for the new quadruplet definition (8), becomes (see T03 for details):

$$\begin{pmatrix} \delta S_{\mathrm{nl},1} \\ \delta S_{\mathrm{nl},2} \\ \delta S_{\mathrm{nl},3} \\ \delta S_{\mathrm{nl},4} \end{pmatrix} = \sum_{j=1}^{N} \frac{1}{2N} \begin{pmatrix} -1 \\ -1 \\ 1 \\ 1 \end{pmatrix} g^{-4} f^{11} \left[\frac{F_1 F_2}{(1-\mu^2)^4} \left(\frac{C_3' F_3}{(1+\lambda)^4} + \frac{C_4' F_4}{(1-\lambda)^4} \right) - \frac{F_3 F_4}{(1-\lambda^2)^4} \times \left(\frac{C_1' F_1}{(1+\mu)^4} + \frac{C_2' F_2}{(1-\mu)^4} \right) \right], \tag{9}$$

where the normalization takes place with a factor $2N$ instead of N, because the new quadruplet has 4 rather than 2 solutions. C_1' through C_4' are constants to be chosen by optimization. With $\mu = 0$, $N = 1$ and

$$C_1' = C_2' = C_3' = C_4' = C, \tag{10}$$

this expanded DIA defined by Eqs. (2), (3), (8) and (9) reduces to the original DIA. The Ueno and Ishizaka (1997) form of the term in square brackets in Eq. (9) is reproduced by choosing

$$C'_3 = C'_4 = C_1, \quad C'_1 = C'_2 = C_2. \tag{11}$$

Webb (1978) makes a distinction between a 'pumping' and a 'diffusion' term in the nonlinear interactions. Tuning these terms individually corresponds to choosing

$$C'_1 = C'_3 = C_3, \quad C'_2 = C'_4 = C_4. \tag{12}$$

This approach has not been used before. There seems to be no justification in literature or theory to separately define all four constants C'_i.

In essence, the above extensions to the original DIA are taken from literature. A new approach is also introduced here. All DIAs retain their basic conservation characteristics within the local contributions for each discrete spectral component considered (as discussed below Eq. (6)). Without loss of these characteristics, it is therefore possible to vary the free parameters in the DIA in spectral space. It is well known that dominant wavenumber scales of interactions vary throughout the spectrum (e.g., Hasselmann, 1963b; Hasselmann and Hasselmann, 1985), particularly with frequency f. This suggests that optimum values of λ and μ should at least be a function of f. It then is only logical to also allow C to vary. The approach where parameters defining the DIA are allowed to vary in spectral space will henceforth be denoted as the Variable DIA.

Using the above rationale, a plethora of single, multiple and variable DIAs can be constructed. However, the optimal DIA needs to have a balance between economy and accuracy. Potential economy can therefore be used to select possibly useful DIAs.

Obviously, the most economical DIAs will be optimized DIAs with a single representative quadruplet, and with tunable constants that are constant in spectral space. Similar DIAs with several representative quadruplet configurations are also economically feasible on modern computer hardware (Hashimoto and Kawaguchi, 2001; Van Vledder, 2001, and corresponding oral presentations at the 2002 WISE meeting). To distinguish these DIAs from the above defined original DIA, they will be denoted here as Multiple DIAs (MDIA), with the understanding that this group of MDIAs includes optimized DIAs with a single component ($N = 1$).

In a Variable DIA, a massive amount of flexibility can be added in spectral space. If such a DIA cannot produce good results for single component DIAs, a MDIA as suggested above is probably more reasonable to use than a Multiple Variable DIA. Hence, only single component Variable DIAs will be considered. Such a DIA will be denoted as a VDIA.

3. Numerical experiments

Two groups of numerical experiments have been performed. In the first set of tests, a single test spectrum is considered, to intercompare the potential of several MDIAs and VDIAs. The test spectrum consists of a standard JONSWAP spectrum (Hasselmann et al., 1973), with a peak enhancement factor $\gamma = 2$, and with the directional distribution of Hasselmann et al. (1980) (see T03 for details). The test spectrum is normalized, so that the peak frequency $f_p = 1$, the peak direction $\theta_p = 0°$, and the spectral density $F(f_p, \theta_p) = 1$. The spectral space is discretized using 36 directions ($\Delta\theta = 10°$) and with a relative frequency increment of 7%. The frequency space is described with 31 discrete frequencies ranging from 0.48 to 3.6 (normalized).

For this test spectrum, the 'exact' nonlinear source term S_{nl} is calculated according to the Webb–Resio–Tracy (WRT) method (Webb, 1978; Tracy and Resio, 1982; Resio and Perrie, 1991), using version 4 of the portable S_{nl} package developed by Van Vledder (2002). For the various DIAs, optimal parameters are estimated by minimizing the rms error ϵ,

$$\epsilon = \sqrt{\int\int (X_{nl}(f,\theta) - S_{nl}(f,\theta))^2 \,\mathrm{d}f\,\mathrm{d}\theta}, \tag{13}$$

where X_{nl} represent the exact source term, and S_{nl} represents the approximation by the DIA considered. Details of the optimization techniques can be found in Appendices A and B of T03. The resulting error of each optimized DIA is normalized with the corresponding error of the original DIA. This normalized error is denoted as ϵ_n. As will be illustrated below, this quantitative measure for accuracy does not always paint a complete picture of the quality of a DIA. Therefore, visual inspection of all resulting source terms is also important.

The inverse modeling experiments with the MDIA consider increasingly complex configurations, as identified in Table 1, focusing on the incremental benefit of increasingly complex configurations. The inverse modeling experiments with the VDIA start from complex configurations, to first establish that the VDIA indeed can produce arbitrary accuracy. After this has been established, the allowed variability of the free parameters in the VDIA is incrementally reduced, to assess the potential of more practical VDIAs. A full account of all test results can be found in T03. For conciseness, only selected results are presented here.

At the conclusion of the first set of tests, the most promising MDIA and VDIA are selected. In the second group of tests, these parameterizations are applied to a set of 20 test cases. These test cases are generated by varying the parameters defining the spectrum and directional distribution of the first test. Furthermore, some spectra with the bimodal directional distribution of Ewans (1998), and with a directional shear are added. Details of these 20 cases can be found in T03. Two versions of the selected MDIA and VDIA are applied to this set of test cases. The first is the version of the parameterization as obtained for the first test. These versions are denoted as the

Table 1
Summary of inverse modeling experiments performed in the first set of tests. Cases M1–4 consider the MDIA. Cases V1–5 consider the VDIA. [μ] identifies that μ is either optimized or 0

Case	N	Optimize	Remarks
M1	1	λ, [μ], C	
M2	2–5	λ, [μ], C	
M3	1	λ, [μ], (C_1, C_2) or (C_3, C_4)	
M4	2–5	λ, [μ], (C_1, C_2) or (C_3, C_4)	
V1		$C(f,\theta)$ unconstrained	$\lambda = 0.25$, $\mu = 0$
V2		$C(f)$ unconstrained	λ, [μ] from M1
V3		$C(f)$ as polynomial of order 1–4	λ, [μ] from M1
V4		$\lambda(f)$, [$\mu(f)$] unconstrained $C(f)$ constant or 2nd order polynomial	
V5		$\lambda(f)$, [$\mu(f)$] as Pade functions. $C(f)$ constant or 2nd order polynomial	

'frozen' MDIA or VDIA. The second is an MDIA or VDIA as optimized for the test case under consideration (denoted as the optimized MDIA or VDIA). There are two reasons for performing the second set of experiments. First, they can be used to assess if the first test case is representative. Second, they can identify if dynamical estimates of parameters can be beneficial for an MDIA or a VDIA.

4. Results

4.1. Single test case

The spectrum and exact (WRT) nonlinear source term $S_{\mathrm{nl}}(f,\theta)$ for the first test are presented in Fig. 1a and b, respectively. The corresponding one-dimensional source term $S_{\mathrm{nl}}(f) = \int S_{\mathrm{nl}}(f,\theta)\,\mathrm{d}\theta$ is shown as the solid or green line in Fig. 1c. The latter figure shows the trademark positive–negative–positive signature for low, intermediate, and high frequencies, respectively. Fig. 1b furthermore shows a tendency of the exact source term to broaden the directional distribution of

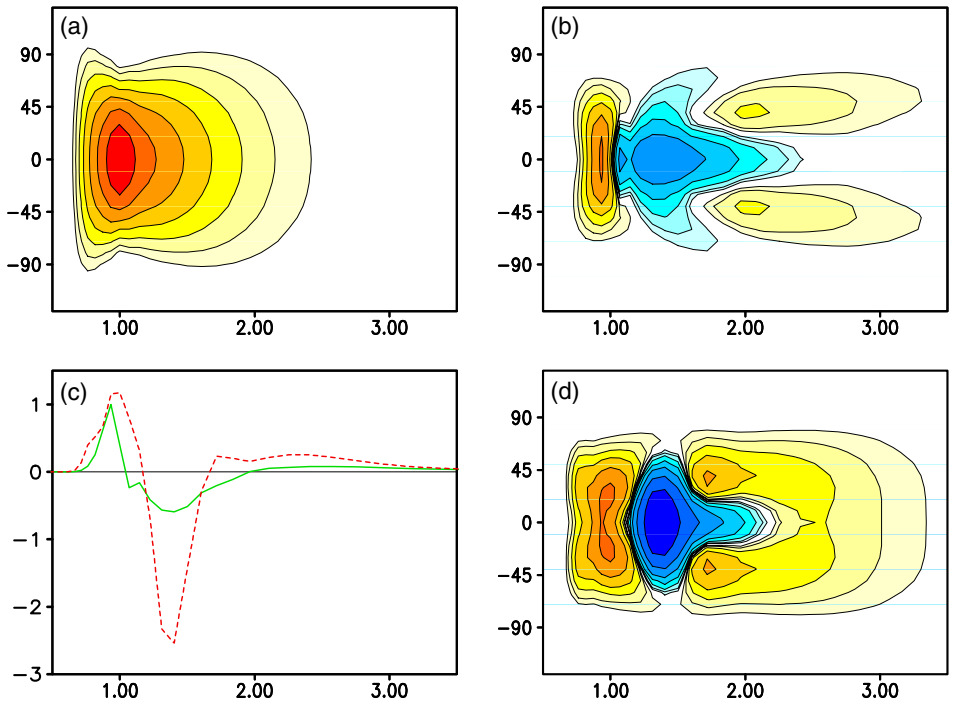

Fig. 1. First test case. (a) Spectrum, logarithmic scaling with factor 2 increment between contours, highest contour at 0.5. (b) Exact interactions according to WRT method. Logarithmic scaling with factor 2 increment, lowest absolute contour value at ±70, blue shading or dashed contours identify negative values. (d) Corresponding results of DIA. (c) One-dimensional interaction $S_{\mathrm{nl}}(f)$, normalized with maximum of $S_{\mathrm{nl}}(f)$ for WRT method. Solid or green lines represent WRT, dashed or red lines represent DIA.

the spectrum for high frequencies ($S_{nl} < 0$ for $f > 1$ and $\theta \approx 0°$, $S_{nl} > 0$ for $f > 1$ and angles away from 0°), as has been observed for many other test spectra.

The nonlinear interaction source term S_{nl} according to the DIA (Fig. 1d) deviates significantly from the exact interactions (Fig. 1b). First, the DIA results in interactions that are too strong. Second, the positive lobe at low frequencies is too broad in frequency space, particularly away from $\theta = 0°$. Third, the positive lobes at high frequencies are shifted in frequency space. Note that the one-dimensional source term (Fig. 1c) describes the positive lobe at low frequencies reasonably well. Hasselmann et al. (1985) chose λ and C to achieve this, because this part of S_{nl} is believed to be crucial for wave growth.

Fig. 2 shows selected cases of the MDIA tests M1 through M4. These illustrations have been selected to highlight shortcomings and potential of several approaches. Fig. 2a shows results of an MDIA with 4 components ($N = 4$), with the original layout of the quadruplet ($\mu \equiv 0$), and with a single constant C (from experiment M2). This approach shows a massive improvement over the original DIA, reducing its error by more than a factor of 5 ($\epsilon_n = 18.6\%$). The positive lobe at low frequencies is much narrower in frequency space for θ close to 0°, than for the original DIA (compare Fig. 1d). However, this approach retains some qualitative shortcomings. For directions away from the mean directions (e.g., $\theta = \pm 45°$), this positive lobe at low frequencies remains

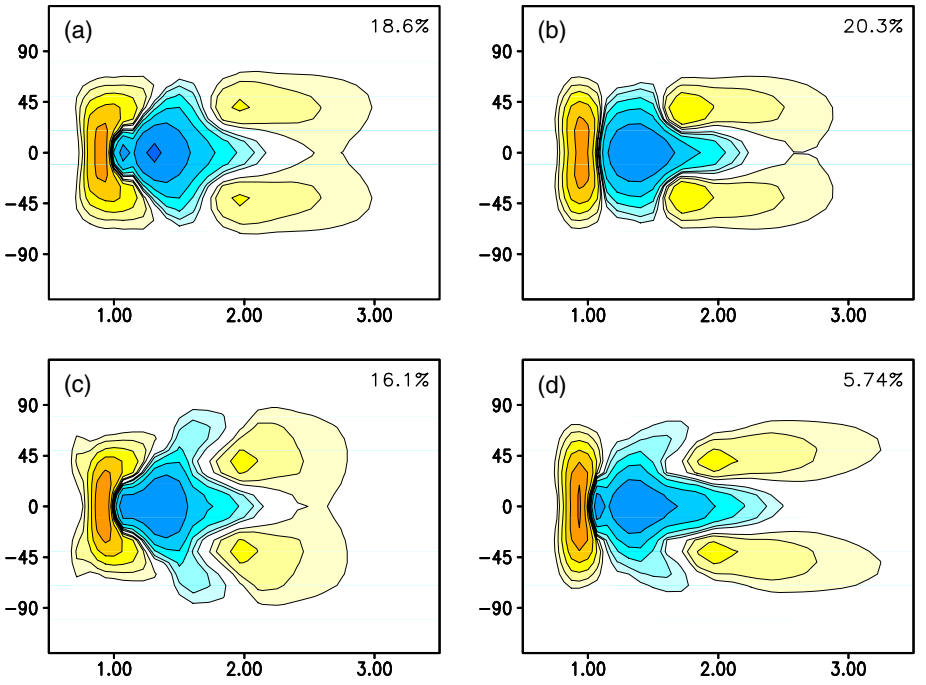

Fig. 2. Nonlinear interaction source term according to selected MDIAs for the first test case. (a) MDIA with four components, original quadruplet definition ($\mu \equiv 0$) and single constant as in Eq. (10). (b) MDIA with one representative quadruplet, λ, μ, and C optimized (cf. Eq. (10)). (c) Like panel (a) but with separate constants C_1 and C_2 as in Eq. (11). (d) MDIA with four components, expanded quadruplet definition (λ and μ, optimized) and single constant as in Eq. (10). Resulting optimum parameters as in Table 2. Legend as in Fig. 1b. Normalized error ϵ_n in upper right corner of each panel.

unrealistically broad in frequency space, when compared to the exact solution (Fig. 1b). This spurious horseshoe shape of the positive lobe of $S_{\mathrm{nl}}(f,\theta)$ at low frequencies remains when the number of components in this MDIA is increased, as long as the original layout of the quadruplet is used ($\mu \equiv 0$).

The shape errors for the positive lobe at low frequencies disappear if the new quadruplet layout is used. This is illustrated in Fig. 2b, which shows results of a single MDIA ($N = 1$), with the expanded quadruplet definition ($\mu \neq 0$), and with a single constant C (Eq. (10), experiment M1). Thus, even if only one component is used in this MDIA, the qualitative description of the source term is better than for the four component MDIA with the traditional definition of the quadruplet (compare with Fig. 2a). Even quantitatively, the latter one-component MDIA is nearly as accurate as the former four-component MDIA. Consequently, it appears crucial to expand the definition of the quadruplet.

Fig. 2c shows results of an MDIA with 4 components ($N = 4$), with the original layout of the quadruplet ($\mu \equiv 0$), and with separate constant C_1 and C_2 (Eq. (11), experiment M4). With the exception of the use of C_1 and C_2, this MDIA is identical to the MDIA presented in Fig. 2a. The introduction of additional tunable constants C_1 and C_2 has a moderate impact on the accuracy of this MDIA, reducing the relative error ϵ_n from 18.6% in the case with a single constant C (Fig. 2a), to 16.1% in the corresponding case with constants C_1 and C_2 (Fig. 2c). The increase of accuracy appears to be accompanied by a more noisy representation of S_{nl}. For some cases, this even leads to spurious wiggles at low frequencies (see T03). The moderate quantitative improvement, combined with a negative qualitative impact, does not seem to justify the complications introduced in the MDIA by adding more tunable constants C_n.

Fig. 2d shows results of an MDIA with four components, an expanded definition of the quadruplet, and a single constant C as in Eq. (10). The corresponding values of coefficients are presented in Table 2. A comparison with Fig. 1b shows an excellent reproduction of the exact interactions, with a reduction of the error compared to the original DIA of a factor of 17 ($\epsilon_n = 5.74\%$). Adding more components has been found to have only a small impact on the error ϵ_n. Moreover, the optimization will then results in quadruplets with nearly identical layout (λ and μ), but with large values of C with opposing signs.

Fig. 3 shows selected cases of the VDIA tests V1 through V5. As in Fig. 2, these illustrations have been selected to highlight shortcomings and potential of several approaches. In the first VDIA experiment (V1), C is allowed to vary in full spectral space without constraints for a given λ and μ (see Table 1). This test was performed to confirm that such a VDIA can reproduce the exact interactions with negligible error, and to assess the structure of the resulting $C(f,\theta)$. Such a VDIA indeed can reproduce the exact interactions (see T03, Fig. 3.9). However, the complexity of the resulting $C(f,\theta)$ is similar to the complexity of the actual interactions. This approach therefore

Table 2
Optimum parameter settings for four component MDIA ($N = 4$) in first test

Component	λ	μ	C
1	0.075	0.023	8.36×10^{7}
2	0.219	0.127	7.28×10^{7}
3	0.299	0.184	3.34×10^{7}
4	0.394	0.135	2.57×10^{6}

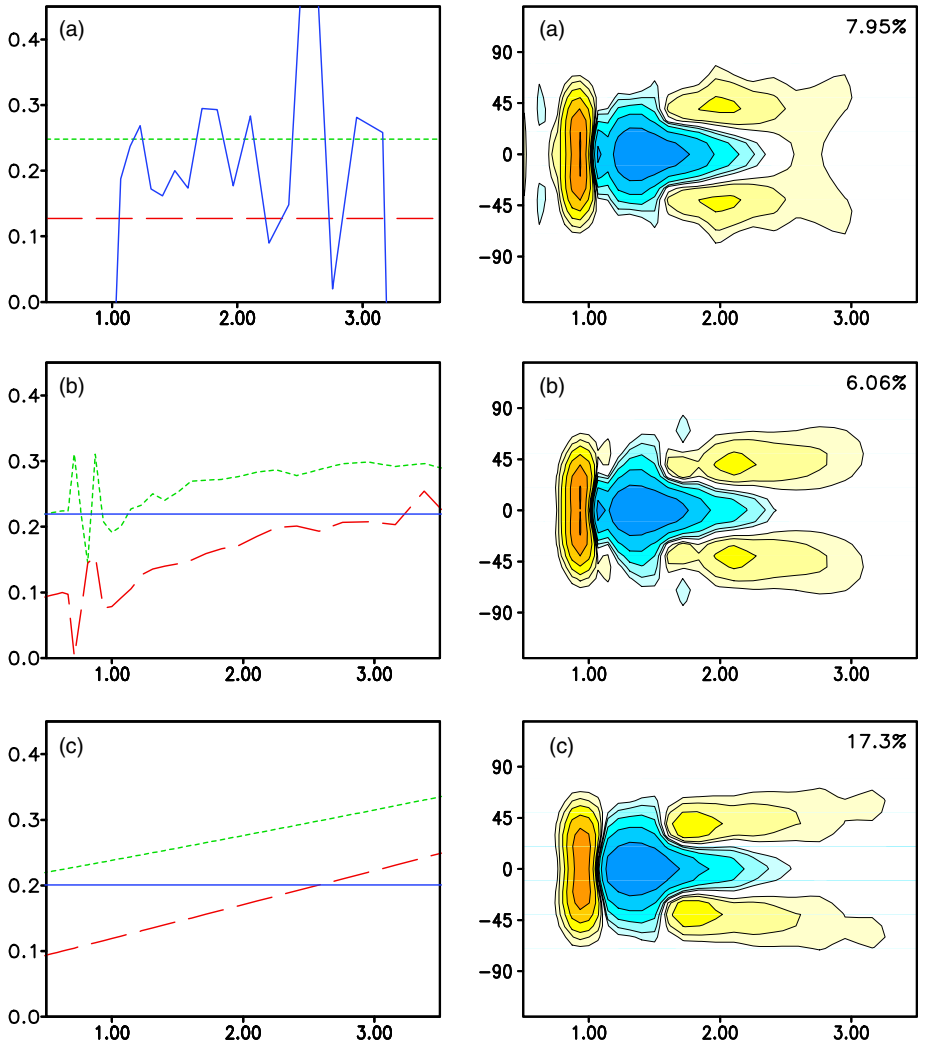

Fig. 3. Nonlinear interaction source term according to selected VDIAs for the first test case, with λ, μ and C as a function of the frequency f only. (a) $\lambda = 0.248$, $\mu = 0.127$ and $C(f)$ optimized without constraints. (b) $\lambda(f)$ and $\mu(f)$ optimized without constraints, C constant but optimized. (c) $\lambda(f)$ and $\mu(f)$ as Pade functions, C constant, all optimized (see Table 3). Left panels show $\lambda(f)$ as short dashed (green) line, $\mu(f)$ as long dashed (red) line, and 10^8 $C(f)$ as solid (blue) line. Right panels show resulting source term, with legend as in Fig. 1b. Normalized error ϵ_n in upper right corner of right panels.

does not provide a practical alternative to calculate S_{nl}. For a practical VDIA, it is necessary to limit the variability of λ, μ and C. A first step in this direction is to allow these parameters to vary with the spectral frequency f only, as justified in the Section 2. Fig. 3 presents a few selected results from several such VDIAs.

Fig. 3a shows results of a VDIA where $C(f)$ is optimized without constraints, and λ and μ, are taken from the corresponding MDIA with $N = 1$ in Table 1 and Fig. 2b (MDIA experiment Ml

and VDIA experiment V2). Allowing $C(f)$ to vary without constraint reduces the error of the resulting DIA by a factor of 2.5 (from $\epsilon_n = 20.3\%$ for a constant C to 7.95% for $C(f)$). However, the qualitative improvement is less impressive, because the resulting source term S_{nl} is clearly noisy (Fig. 3a). Moreover, $C(f)$ itself (solid blue line in left panel of Fig. 3a) displays large variability, and hence shows little promise for practical modeling of S_{nl}.

Fig. 3b shows results of a VDIA in which $C(f)$ is an optimized constant, and $\lambda(f)$ and $\mu(f)$ are optimized without constraints (experiment V4). This VDIA shows marginally better quantitative behavior than the previously discussed VDIA, with an improvement of the normalized error of a factor of 16.5 compared to the original DIA, and a factor of 3.3 compared to the corresponding optimum single component MDIA of Fig. 2b. However, the improvement is again not as large in a qualitative sense, due to the noisy character of S_{nl} (right panel of Fig. 3b). Nevertheless, $\lambda(f)$ and $\mu(f)$ in this VDIA are much better behaved than $C(f)$ in the previously discussed VDIA for most of the frequency range (compare left panels in Fig. 3a and b). This suggests that a simple functional description of $\lambda(f)$ and $\mu(f)$ could result in a systematic improvement of the VDIA compared to the corresponding MDIA. The advantages of such an approach are that first, the corresponding VDIA is more feasible, due to a smaller number of free parameters, and second, that smooth estimates of $\lambda(f)$ and $\mu(f)$ are tentatively expected to result in a less noisy representation of S_{nl}. Fig. 3c show the results obtained by using a representation based on a Pade function approach for $\lambda(f)$ and $\mu(f)$. The functional description chosen here for the Pade function representation is given by

$$P(f) = \frac{a_0 + a_1 f}{1 + a_2 f}, \tag{14}$$

where a_0 through a_2 are the tunable constants. The corresponding VDIA with a single constant C is shown in Fig. 3c, and its coefficients are presented in Table 3. This VDIA shows only a moderate quantitative improvement over the corresponding MDIA of Fig. 2b ($\epsilon_n = 17.3\%$ vs. 20.3%,). However, the qualitative improvement is notable, and this version of the VDIA does not show the noisy behavior as is displayed for the unconstrained λ and μ in Fig. 3b. This VDIA can probably be improved by choosing a more appropriate functional description of $\lambda(f)$ and $\mu(f)$, as will be discussed in Section 5. However, for the present feasibility study, the Pade description will be considered adequate to assess the concept of this VDIA.

4.2. Multiple test cases

A fairly representative example of the results of the second set of test cases is presented in Fig. 4. The test spectrum (case 19 of T03) is mildly sheared, with an asymmetric bimodal directional

Table 3
Optimum Pade coefficients of Eq. (14) for VDIA in the first test

Parameter	a_0	a_1	a_2
λ	0.202	0.0323	−0.0170
μ	0.0681	0.0506	−0.00377
C	2.007×10^7	0	0

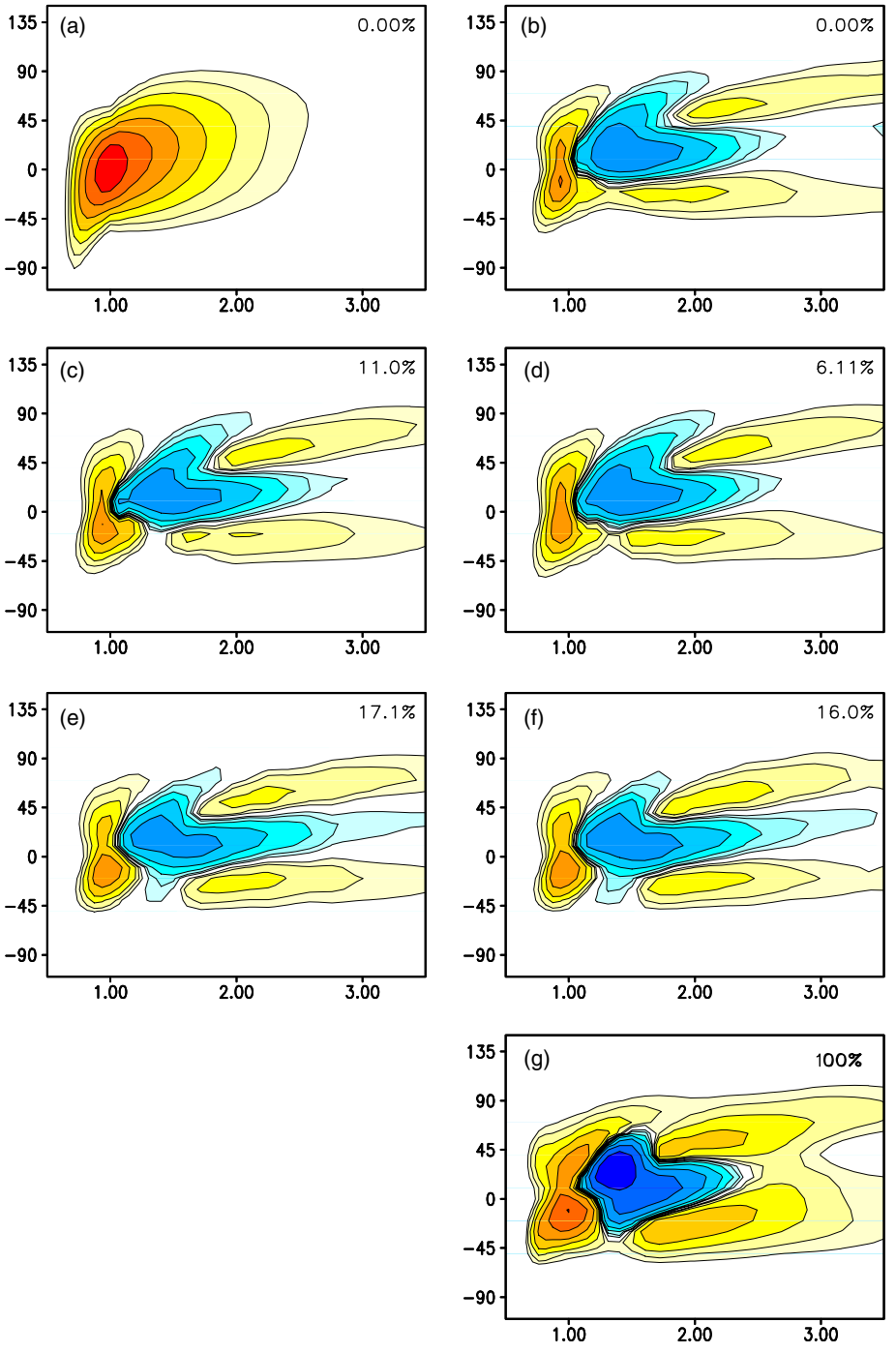

Fig. 4. Nonlinear interaction source term according to several algorithms for case 19 of second sets of test. (a) Spectrum, (b) exact (WRT) source term, (c) frozen MDIA, (d) optimal MDIA, (e) frozen VDIA, (f) optimal VDIA, (g) original DIA. Legend as in Fig. 1a and b. Note that scaling differs from Fig. C.19 of T03. Normalized errors ϵ_n in upper right corner of panels.

distribution. The frozen MDIA (Fig. 4c), closely resembles the exact solution (Fig. 4b). The optimized MDIA (Fig. 4d) is significantly more accurate, and, for all practical purposes, reproduces the exact interactions. The frozen VDIA (Fig. 4e) is less accurate, but represents a major improvement over the original DIA, reducing the error by a factor of more than 5. The optimized VDIA (Fig. 4f) shows marginally more accurate results. A main qualitative shortcoming of the VDIA is the lack of asymmetry for higher frequencies ($f > 1.5$). The VDIA appears to share this deficiency with the original DIA. The original DIA (Fig. 4g) has all quantitative and qualitative shortcomings that were identified in the first test.

Fig. 5 summarizes the results of all test cases. Panel (a) presents the normalized error ϵ_n of the optimized models as a function of the corresponding errors of the frozen models, for all cases, and for both the MDIA and the VDIA. Panel (b) shows the relative improvement of the MDIA and VDIA due to the case-by-case optimization as a function of the errors of the frozen model. Several conclusions can be drawn from this figure.

First, both the MDIA and VDIA generally behave significantly better than the original DIA, with virtually all errors $\epsilon_n < 1$, and most errors $\epsilon_n \ll 1$ (Fig. 5a). Although no comparison between the MDIA and VDIA is presented on a case-by-case basis, it is also obvious from Fig. 5 that the MDIA systematically produces better results that the VDIA (i.e., smaller errors ϵ_n).

Second, for three outlying cases, the VDIA shows only marginal improvement over the original DIA, even in its optimized form ($\epsilon_n > 0.6$, Fig. 5a). As can be seen in the individual test results presented in T03, these cases all consider sharply peaked spectra. In these cases, the qualitative improvement provided by the VDIA appears more significant than the quantitative improvement (see T03). Furthermore, the reduction in error by optimizing the VDIA is generally small, with a corresponding reduction of the error by less than 20% for 15 of the 20 cases (Fig. 5b). Since 2 of the 5 cases with larger impact consider sharply peaked spectra which are poorly treated by the VDIA, and 1 such case is already accurately depicted by frozen VDIA, it appears that there is little benefit in dynamically estimating free parameters of the present VDIA.

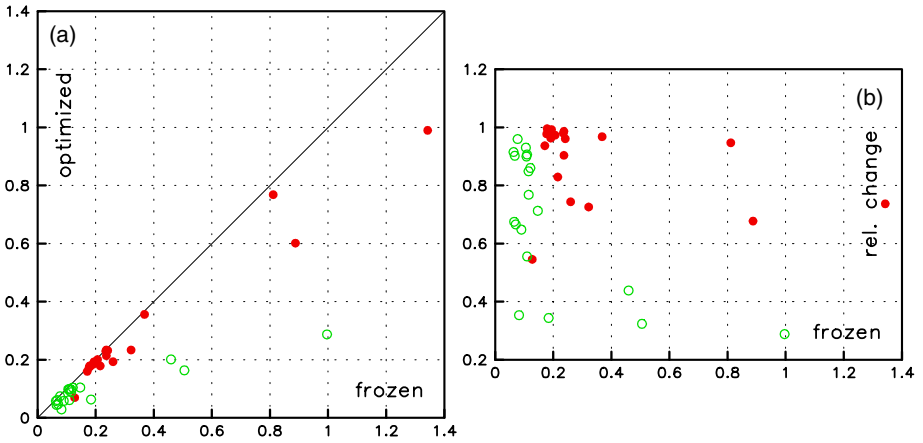

Fig. 5. Resulting normalized errors ϵ_n for all test cases, (a) Error of optimized model as a function of the error of the frozen model. (b) Relative change in error defined as error of optimized model normalized with error of frozen model, as a function of the latter. MDIA: open green circles. VDIA: solid red circles. (Fig. 4.1 from T03.)

Third, the optimized MDIA shows a large improvement over the original DIA with $\epsilon_n < 0.3$ for all cases, and $\epsilon_n < 0.1$ for 14 out of 20 cases (Fig. 5a). Furthermore, the impact of the optimization is much larger for the MDIA than for the VDIA, with an error reduction due to the optimization of more than 25% for 10 cases, and more than 50% for 5 cases (Fig. 5b). Hence, the MDIA has a much higher potential to benefit from dynamical estimation of parameters than the VDIA.

5. Discussion

The present study investigates the potential of several previously published Discrete Interaction Approximations (DIAs) for the nonlinear interactions in wind wave spectra. Inverse modeling, where the free parameters in the different DIAs are objectively estimated by fitting the DIA to the exact solution, indicates that the accuracy of the original DIA is mostly constrained by the limited flexibility of the layout of its representative quadruplet. In the original approach of Eqs. (2), (3), and (5), only one free parameter governs the layout of the representative quadruplet. Van Vledder (2001) suggests an alternative layout of the quadruplet using three free parameters. This definition of the quadruplet can reproduce any possible quadruplet. In the present study a two-parameter quadruplet layout is suggested (Eq. (8)), which retains some, but not all, of the versatility of Van Vledder's approach. Results presented here indicate that this expanded flexibility of the representative quadruplet is essential for a DIA to be able to accurately reproduce the exact interactions. The new two-parameters quadruplet appears to have sufficient flexibility for accurate representation of exact interactions for individual spectra.

Ueno and Ishizaka (1997) advocate the addition of more proportionality constants C_i' to the original DIA, cf. Eq. (9). The present study indicates that this modification of the DIA has a limited quantitative impact on the accuracy of the DIA. It furthermore appears to add noise to the resulting source term S_{nl}. Consequently, this modification does not appear justified based on quantitative measures, and may even be detrimental in a qualitative sense.

Considering the above, the optimal form of the DIA includes the new quadruplet layout of Eq. (8), and a single proportionality constant as in Eqs. (9) and (10). This DIA benefits greatly from a multiple DIA (MDIA) approach with more than one representative quadruplet. Using four representative quadruplets, the resulting source term S_{nl} (Fig. 2d) becomes virtually indistinguishable from the exact source term (Fig. 1b). Adding more than four quadruplets has a limited incremental impact on the accuracy of the MDIA (T03, Table 3.1). Moreover, for larger numbers of quadruplets in the MDIA near-identical quadruplets (i.e., λ and μ) are found with constants C with opposite signs. Hence differences between (near-identical) contributions rather than individual contributions of quadruplets start to dominate the incremental improvement. It is not likely that such contributions can result in systematic model improvement for arbitrary spectra. It therefore appears that the present MDIA, where the quadruplet layout is allowed to vary without restrictions in the optimization, may be expected to show optimal results for approximately four components.

Fig. 5 indicates that the above MDIA with four components might benefit significantly from a dynamic estimate of its free parameters, based on characteristics of the actual spectrum considered. Such results might be anticipated because Hashimoto and Kawaguchi (2001) have already

shown that the optimum parameters for a single MDIA are a distinct function of the shape of the spectrum.

The present study introduces the concept of a Variable DIA, where the parameters λ and μ, defining the quadruplet, as well as the proportionality constant C are allowed to vary in spectral space. Such an approach in general can produce accurate estimates of the source term S_{nl}, but tends to do so at the expense of noise in S_{nl}. Furthermore, these parameters themselves tend to show significant variability, limiting the practical applicability of such an approach.

To obtain a practical VDIA, λ, μ and C are allowed to vary with the spectral frequency f only. This is consistent with the observation that the dominant scale of interactions typically is a function of f, as is discussed in Section 2. Experiments with unrestrained optimization of $C(f)$ result in a noisy optimal C (Fig. 3a), with little hope for a practical parameterization. A practical VDIA should therefore use a constant and optimized C. Such a VDIA with unrestrained $\lambda(f)$ and $\mu(f)$, results in fairly well behaved optimum parameters (Fig. 3b), which could be described with simple functions. A first practical VDIA then was obtained with a constant C, and with Pade functions describing λ and μ. Such a VDIA proved qualitatively about 15% more accurate than the corresponding MDIA with one component. More importantly, it appears qualitatively more sound (Fig. 3c).

A close comparison of Fig. 3b and c reveals that the Pade description of λ and μ results in a spurious shift of the positive lobes at high frequencies to lower frequencies. This deficiency is shared with the single MDIA (Fig. 2b). In this frequency range, the unrestrained λ and μ are well behaved, and differ clearly from the Pade estimates. It may therefore be expected that alternatives to the Pade description, which follow the unrestrained estimates more closely, would significantly improve the behavior of this VDIA at higher frequencies. The Pade based VDIA furthermore underestimates the magnitude of the positive lobe at low frequencies. In this frequency range, the unrestrained λ and μ show great variability. It is therefore not expected that alternatives to the Pade function can improve the behavior of the VDIA for low frequencies.

Application of the Pade function based VDIA to a larger set of test cases, shows that this VDIA is not particularly accurate for sharply peaked spectra. A positive attribute of this VDIA is that it benefits little from optimization for individual cases. This implies that the 'frozen' VDIA is more generally applicable than other versions of the DIA considered in this study.

6. Conclusions

The present study investigates the potential of previously suggested and some new Discrete Interaction Approximations (DIAs) for nonlinear interactions for wind waves to accurately depict the corresponding source term S_{nl} for selected wind wave spectra. It is shown that it is crucial to expand the definition of the representative quadruplet to gain accuracy. Adding more constants to the calculation of the strength of discrete interactions has insufficient positive impact to justify this complication of the algorithm. A Multiple DIA (MDIA) with an expanded quadruplet definition and about four representative quadruplets is shown to reproduce the exact source term adequately. This MDIA would benefit from a dynamic estimation of its free parameters as a function of characteristics of the spectrum such as the spectral shape. A new Variable DIA (VDIA) is

introduced, where the free parameters in the representation are allowed to vary as a function of the spectral frequency f. This new VDIA is less accurate but cheaper than the MDIA.

Acknowledgements

The author would like to thank Henrique Alves and D.B. Rao, for their comments on early drafts of this manuscript. This study was supported by funding from the Office of Naval Research under grant N00014-00-F-0332, and by funding from the NOAA High Performance Computing and Communication (HPCC) office.

References

Ewans, K.C., 1998. Observations of the directional spectrum of fetch-limited waves. Journal of Physical Oceanography 28, 495–512.

Hashimoto, N., Kawaguchi, K., 2001. Extension and modification of Discrete Interaction Approximation (DIA) for computing nonlinear energy transfer of gravity wave spectrum. In: Ocean Wave Measurement and Analysis. ASCE, pp. 530–539.

Hasselmann, D.E., Dunckel, M., Ewing, J.A., 1980. Directional wave spectra observed during JONSWAP 1973. Journal of Physical Oceanography 10, 1264–1280.

Hasselmann, K., 1960. Grundgleichungen der seegangsvoraussage. Schiffstechnik 1, 191–195.

Hasselmann, K., 1962. On the non-linear transfer in a gravity wave spectrum. Part 1. General theory. Journal of Fluid Mechanics 12, 481–500.

Hasselmann, K., 1963a. On the non-linear transfer in a gravity wave spectrum. Part 2. Conservation theory, wave-particle correspondence, irreversibility. Journal of Fluid Mechanics 15, 273–281.

Hasselmann, K., 1963b. On the non-linear transfer in a gravity wave spectrum. Part 3. Evaluation of energy flux and sea-swell interactions for a Neuman spectrum. Journal of Fluid Mechanics 15, 385–398.

Hasselmann, K., Barnett, T.P., Bouws, E., Carlson, H., Cartwright, D.E., Enke, K., Ewing, J.A., Gienapp, H., Hasselmann, D.E., Kruseman, P., Meerburg, A., Mueller, P., Olbers, D.J., Richter, K., Sell, W., Walden, H., 1973. Measurements of wind-wave growth and swell decay during the Joint North Sea Wave Project (JONSWAP). Ergaenzungsheft zur Deutschen Hydrographischen Zeitschrift, Reihe A(8) 12, 95.

Hasselmann, S., Hasselmann, K., 1985. Computations and parameterizations of the nonlinear energy transfer in a gravity-wave spectrum. Part I: A new method for efficient computations of the exact nonlinear transfer integral. Journal of Physical Oceanography 15, 1369–1377.

Hasselmann, S., Hasselmann, K., Allender, J.H., Barnett, T.P., 1985. Computations and parameterizations of the nonlinear energy transfer in a gravity-wave spectrum. Part II: Parameterizations of the nonlinear energy transfer for application in wave models. Journal of Physical Oceanography 15, 1378–1391.

Herterich, K., Hasselmann, K., 1980. A similarity relation for the nonlinear energy transfer in a finite-depth gravity-wave spectrum. Journal of Fluid Mechanics 97, 215–224.

Komen, G.J., Cavaleri, L., Donelan, M., Hasselmann, K., Hasselmann, S., Janssen, P.E.A.M., 1994. Dynamics and Modelling of Ocean Waves. Cambridge University Press. p. 532.

Masuda, A., 1980. Nonlinear energy transfer between wind waves. Journal of Physical Oceanography 10, 2082–2093.

Phillips, O.M., 1960. On the dynamics of unsteady gravity waves of finite amplitude. Journal of Fluid Mechanics 9, 193–217.

Phillips, O.M., 1981. Wave interactions: the evolution of an idea. Journal of Fluid Mechanics 106, 215–227.

Resio, D.T., Perrie, W., 1991. A numerical study of nonlinear energy fluxes due to wave–wave interactions. Part 1: Methodology and basic results. Journal of Fluid Mechanics 223, 609–629.

SWAMP group, 1985. Ocean Wave Modelling. Plenum Press. p. 256.

Tolman, H.L., 2003. Optimum Discrete Interaction Approximations for wind waves. Part 1: Mapping using inverse modeling. Tech. Note 227, NOAA/NWS/NCEP/MMAB, 57 pp. + Appendices.

Tracy, B., Resio, D.T., 1982. Theory and calculation of the nonlinear energy transfer between sea waves in deep water. WES Report 11, US Army Corps of Engineers.

Ueno, K., Ishizaka, M., 1997. On an efficient calculation method of the nonlinear energy transfer in wind waves. Sottukojiho, JMA 64, 75–80 (In Japanese).

Van Vledder, G.Ph., 2001. Extension of the Discrete Interaction Approximation for computing nonlinear quadruplet wave–wave interactions in operational wave prediction models. In: Ocean Wave Measurement and Analysis. ASCE, pp. 540–549.

Van Vledder, G.Ph., 2002. A subroutine version of the Webb/Resio/Tracy method for the computation of nonlinear quadruplet interactions in a wind-wave spectrum. Report 151b, Alkyon, The Netherlands.

Van Vledder, G.Ph., Herbers, T.H.C., Jenssen, R.E., Resio, D.T., Tracy, B., 2000. Modelling of non-linear quadruplet wave–wave interactions in operational wave models. In: Proceedings 27nd International Conference on Coastal Engineering, Sydney, Australia. ASCE, pp. 797–811.

WAMDIG, 1988. The WAM model—a third generation ocean wave prediction model. Journal of Physical Oceanography 18, 1775–1809.

Webb, D.J., 1978. Non-linear transfers between sea waves. Deep-Sea Research 25, 279–298.

Young, I.R., Van Vledder, G.Ph., 1993. A review of the central role of nonlinear interactions in wind-wave evolution. Transactions of the Royal Society of London 342, 505–524.